ANGEWANDTE
CHEMIE
Volume 26 · Number 6
June 1987
Pages 527–544

International Edition in English

Reprint

The Development of Bioglass Ceramics for Medical Applications

By Werner Vogel* and Wolfram Höland

The enormous progress made in the field of medicine over the past few decades has been partly due to the introduction of new instruments but also a result of the use of new materials. It is impossible to imagine modern medicine without metals, alloys, sintered corundum, organic high polymers (also as composite materials), glassy carbon, etc. Bioglass ceramics open up new possibilities for medical treatment and constitute a new area of research in the natural sciences and medicine. Owing to their widely variable combinations of properties, bioglass ceramics can be more easily adapted to suit medical requirements than can customary implants. Two properties of bioglass ceramics are of primary importance: their biocompatibility, i.e., acceptance of the material by the tissues of the human body without irritation, rejection reactions, or toxic effects; and their bioactivity, i.e., the ability to establish firm intergrowths with tissues of the human body. This property is not shared by any of the classical biomaterials. A wide range of applications is envisaged for the bioglass ceramics that have so far been developed; some are still undergoing animal tests while others are being clinically tested in humans. Possible applications are the replacement of vertebrae and use in the middle ear, throat, nose, and eye, in the entire head region, in the shoulder and leg, and in dental prosthetics, in particular the replacement of dental roots (a hard tissue substitute in the broadest sense of the word). The question as to the behavior of a bone/bioglass ceramic contact or bond on a long-term scale and on being exposed to varying mechanical stress has still not been satisfactorily answered, because interdisciplinary research in this field is still immature. All observations made so far indicate, however, that the materials do not cause any adverse effects.

1. Introduction

The development of new materials for bone implants and substitutes in man has gained major importance over the past five to ten years. In addition to metals, sintered corundum, and organic polymers, bioglasses and bioglass ceramics have come especially to the fore. These new implant materials are not only biocompatible, like the other customary materials, but are also bioactive. They are not regarded as foreign bodies and encapsulated by living bone tissue; instead, direct intergrowth takes place. The special combinations of properties required by medicine can be more easily adjusted and varied in bioglasses and bioglass ceramics than in metals, sintered corundum, or organic polymers. Moreover, bioglasses and bioglass ceramics can be more easily adapted to the natural composition of bone, which obviously adds greatly to their bioactivity and their compatibility with living human tissue. It should be mentioned at this point that some of the uses of these new materials in medicine extend considerably beyond mere bone replacement.

2. Conditions for Controlled Crystallization in Glass as the Basis for the Systematic Development of Glass Ceramics

A review article was published in this journal in 1965 concerning the "Structure and Crystallization Behavior of Glasses."[1] Subsequent studies, which considerably extended these earlier findings, have since been reviewed.[2, 3] They have provided a reliable basis for the development of a large number of new optical and technical glasses, for overcoming disturbances in glass production, and for the development of several families of new glass ceramics with widely differing properties and combinations of properties.

It can be demonstrated experimentally that most phase separations that occur when glass melts solidify to form a solid body produce a microheterogeneous structure. In the simplest case, a droplet-shaped microglass phase is incorporated in a matrix glass phase with a different composition. The resultant microglass phases are not the product of statistical variations in composition; they tend instead to assume a composition corresponding to that of defined, stable chemical compounds—the extent to which this is achieved depends on the degree of undercooling of the melt. Phase separation can be controlled in a multitude of ways and represents the key to the developments cited above. Figure 1a shows a typical example of a phase-separated glass with a microheterogeneous structure.

The reason for phase separation is presumably the presence of at least two different building groups with extremely different volume requirements. This phase separation entails considerable consequences for the crystallization behavior of a glass. (For a theoretical treatment of phase-separation phenomena in glasses, see Ref. [3].)

The theoretical basis for homogeneous nucleation is given by Volmer's equation [Eq. (1)], which states that the nucleation rate I depends primarily on the enthalpy of activation required to attain the critical nuclear size.

[*] Prof. Dr. W. Vogel, Dr. W. Höland
Otto-Schott-Institut der Sektion Chemie der Universität
Fraunhoferstrasse 6, 6900 Jena (GDR)

a)

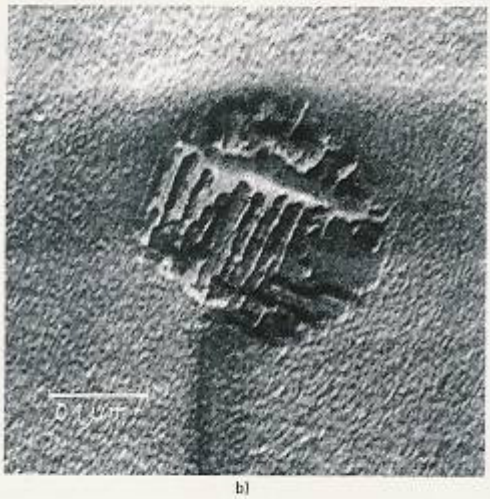

b)

Fig. 1. a) Typical immiscibility phenomena in a silicate glass. Replica electron micrograph of a glass fracture surface prepared in a high vacuum. The droplets with their "fracture flags" are incorporated in a matrix glass phase of different composition. b) The start of nucleation within the droplet region (replica electron micrograph).

$$I = A \cdot e^{-\frac{\Delta G^* + \Delta G_D}{k \cdot T}} \quad (1)$$

A = constant
ΔG^* = enthalpy of activation for reaching the critical nuclear size
ΔG_D = enthalpy of diffusion
k = Boltzmann's constant
T = temperature

The enthalpy of activation consists of two terms ($\Delta G^* + \Delta G_D$). The total activation energy decreases by the amount ΔG_D if the building blocks of the nucleus are already present at the nucleation site. This is the case when phase-separated base glasses are induced to nucleate and crystallize (Fig. 1b). Since the composition of the droplet regions closely approaches that of defined, stable chemical compounds, nucleation begins simultaneously in all of the droplets. The number and size of the resulting crystals can accordingly be varied by controlling phase-separation phenomena in the glass. As is shown in Figure 1b, growth of the crystallite front is stopped when it reaches the droplet phase boundary; i.e., even if nucleation happens to be delayed in one or other of the droplets, the sizes of the crystals will be comparable because growth of the nuclei stops at the droplet boundary. The following main criteria must be satisfied for controlled crystallization in glass: the starting conditions for nucleation should be uniform at an infinite number of equally distributed sites within the total volume of glass and the final product should contain equal-sized crystallites with very small dimensions (usually only a few micrometers).

Heterogeneous nucleation (i.e., nucleation in the presence of a foreign nucleus) is described by Turnbull's relation [Eq. (2)]. Foreign nuclei can be produced in glass in a

$$I = A' \cdot e^{-\frac{(\Delta G^* \cdot f(\theta) + \Delta G_D)}{k \cdot T}} \quad (2)$$

variety of ways. If at least two of their lattice constants do not differ from those of the desired crystalline phase by more than ±15% (or a multiple of the lattice constants of the desired crystalline phase), epitaxial interactions can occur. In other words, the foreign nucleus that has become capable of growth can continue to grow with an unrelated substance, i.e., with the molecular building groups of the desired crystalline phase, which, for example, may be located in the droplets. This also accounts for the fact that it is often very difficult or even impossible to demonstrate and unequivocally identify the heteronuclei in cases of epitaxial interaction. Epitaxy further decreases the necessary critical enthalpy of activation for nucleation, ΔG^*, by a function of θ, $f(\theta)$. It is a function of the measurable contact angle θ between the foreign nucleus and the melt from which the main crystalline phase is to be formed. The contact angle reflects the strength of the epitaxial interaction. If deposition occurs, this function is always less than 1, which means that nucleation and crystallization proceed much more quickly than without a foreign nucleus. The action of foreign nuclei can to some extent be compared with that of initiators.

3. Development of Bioglass Ceramics—Present Status, Requirements, and Our Own Goals

Important advances have been made in the field of medicine as a result of developments generally involving the use of phosphosilicate glasses (which are closely related to the apatite-rich bone substance) to form coatings and thin films on implant materials such as metals and sintered corundum.[4–6] Thin glass films have also been employed which, in some cases, have been converted into crystalline apatite by tempering. These bone-related glasses and glassy crystalline films exhibit relatively good bioactivities and bonding with the bone tissue. As a rule, however, thin films ultimately dissolve and thus become useless. This behavior has been exploited for different purposes to de-

velop completely reabsorbable glasses and glass ceramics.[7-9] Another approach was to develop sintered ceramics as solid materials, usually sintered products consisting of crystalline apatite.[10] Powdered phosphate glasses in which crystalline apatite is formed by tempering have also been used as sintered products.[11,12] The resulting properties were then further modified by sintering mixtures of a phosphate glass powder and a silicate glass powder in which crystalline silicates such as wollastonite or devitrite separate out.[13,14] The products obtained are porous and of variable bioactivity, depending on their apatite content, and can be worked to a limited extent with tools made of hard metals. Their porosity and relatively poor mechanical strength, however, often prove to be serious disadvantages.

An important advance was made when glassy crystalline products were obtained by tempering solid glasses.

The first important step toward the formation of a solid bond between inorganic materials and bone was taken by *Hench* et al. with the preparation of glass films and partially crystalline glasses.[15,16] Their base glass had the following composition [wt%]:

SiO_2	45	CaO	24.5
Na_2O	24.5	P_2O_5	6.0

In the 1970s, the development of the so-called ceravital material (which is based on the base glass system SiO_2-Na_2O-CaO-$Ca_3(PO_4)_2$-MgO-K_2O-CaF_2) led to a significant improvement in chemical stability and thus opened up the way for new applications.[17,18] More recent developments, which are essentially all based on the above base glass system, have brought about further advances.[19-21] Extensive studies, especially on different possible applications, revealed that the bioactivity of these materials was good but that the bonding zone between the bone (or other tissue) and the glassy crystalline material broadened owing to the relatively high solubility of the latter; moreover, this process did not come to a standstill on prolonged contact of the material with the bone. This means that there is a risk that the implant will become loose if the bonding zone is subjected to mechanical stress. The bonding is adequate, however, for other types of applications. The main crystalline phases of the new materials cited are apatite ($Ca_5[F/(PO_4)_3]$), wollastonite ($Ca_2[Si_2O_6]$), and/or devitrite ($Na_2O \cdot 3CaO \cdot 6SiO_2$).

The authors' own aim has been to develop bioglass ceramics with novel properties by using available knowledge about the microprocesses occurring on solidification of a glass melt and during conversion of a glass to a glass ceramic by means of controlled crystallization. The requirements of our meanwhile large number of medical collaborators vary widely; it thus seems likely that a series of bioglass materials will be developed that is to a certain degree comparable with the range of stainless steels now available for various applications. The properties primarily required are:

- complete biocompatibility or
- maximum bioactivity with
  maximum mechanical strength,
  a high degree of chemical resistance, especially against body fluids, and
  good machinability, ideally carried out by the surgeon.

Good biocompatibility means, for example, that cell compatibility tests, both in vitro and in vivo, do not indicate the occurrence of defense reactions or toxic effects and that direct contact is established with the bone without the formation of connective tissue. Bioactivity is understood to be the ability of the implant to stimulate the tissue to form a true biochemical bond with it after a limited period of dissolution and ion exchange.

4. Development of Biocompatible, Machinable Glass Ceramics

4.1. Machinable Glass Ceramics from the System Na_2O-MgO-Al_2O_3-SiO_2-F with Flat, Flake-Shaped Mica Crystals[22]

A glass ceramic is defined as being machinable if it can be turned, milled, drilled, or threaded with metal-working tools (primarily those made of hard metals) without causing the workpiece to fracture as is the case with ordinary ceramics. The test devised to compare machinability involves measuring the time required for a hard-metal drill to penetrate to a specified depth under otherwise identical conditions.

The development made by *Beall* and *Grossmann* et al.[23-25] in the early 1970s entails the controlled separation of mica crystals in a given base glass. In order to ensure good machinability the crystals should be of optimal size, should be in mutual contact, and should account for about two-thirds of the total volume of the ceramic.[3]

Figure 2 shows a typical example of this type of material developed by our group. A standard base glass (15.5 mol%

Fig. 2. Flat sodium phlogopite mica crystals arranged like a "card house" in a machinable glass ceramic (scanning electron micrograph).

MgO, 12.6 mol% Al_2O_3, and 71.9 mol% SiO_2) was used in which 11.2 mol% of the oxygen ions were replaced by fluoride ions and which was additionally doped with 5.2 mol% sodium oxide. By controlled phase separation of the base glass, sodium phlogopite crystals ($Na_{0.5-1}Mg_3[AlSi_3O_{10}F_2]$), a type of mica, were made to separate out in a specific fashion in accordance with the given requirements.[26,27]

The machinability is based on the fact that the microfractures produced by machining occur preferentially along the (001) plane of the mica crystals (see Fig. 3). Since the crystals are in mutual contact, the microfractures readily propagate to neighboring crystals. The material can thus be worked without shattering. The (001) plane of the mica crystal is the preferred direction of fracture owing to the presence of alkali ions (see Fig. 4), which loosely connect two triple-layer packets.

This ceramic, developed for special applications in scientific instruments and mechanical engineering, is also biocompatible and can be used in a variety of ways in medicine. Its physical properties are listed in Table 1.

Table 1. Properties of the machinable glass ceramic containing flat fluorophlogopite mica crystals. Composition [mol%]: Na_2O 3–15, MgO 7–23, Al_2O_3 10–30, SiO_2 45–70, F 3–6 [22].

Density	2.5 g/cm^3
Linear coefficient of thermal expansion (20–400 °C)	75×10^{-7} K^{-1}
Mechanical flex-cracking resistance	90 MPa
Modulus of elasticity	50 GPa
Pressure resistance	450 MPa
Shock resistance	2.0 kN/m
Hydrolytic class	1–2
Acid class	1
Alkali class	1–3
Roughness height after polishing	0.15 μm
Machinability	Very good

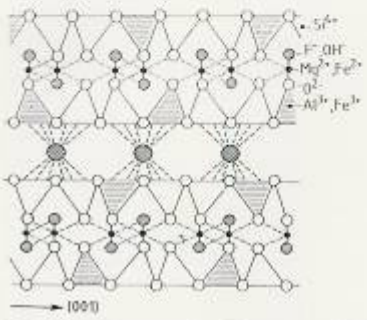

Fig. 3. Schematic representation of the structure of phlogopite. Triangles, $[SiO_4]$ tetrahedra; hatched triangles, $[AlO_4]$ tetrahedra; ● K^+ or Na^+; ○, O^{2-}; ◐, F^-; •, Mg^{2+}. F^- can be replaced by OH^-, Mg^{2+} by Fe^{2+}, Al^{3+} by Fe^{3+}, and K^+ by Na^+.

4.2. Glass Ceramic with Maximum Machinability from the System Na_2O/K_2O-MgO-Al_2O_3-SiO_2-F with Curved Mica Crystals[28,29]

A previously unknown mica phase could be induced to separate in a different standard base glass (21.2 mol% MgO, 19.5 mol% Al_2O_3, 59.3 mol% SiO_2) after doping with 11.2 mol% F^- and 6.4 mol% Na_2O/K_2O. Here, the mica crystals do not occur as flat flakes but as cabbagelike aggregations of curved "leaves" (see Fig. 4). Comparison of the Mg and Al peaks in the X-ray spectra obtained by energy-dispersive electron-beam microanalysis (EDAX)[30] (see Fig. 5) revealed that the Al concentration in the curved mica crystals is higher than that in the flat crystals. Increasing the total (Al_2O_3 + MgO) content of the glass relative to the SiO_2 content results in replacement of part of the Mg^{2+} ions by Al^{3+} ions (1.5 Mg^{2+} correspond to 1 Al^{3+}) in the new mica crystal. As a result, stresses develop

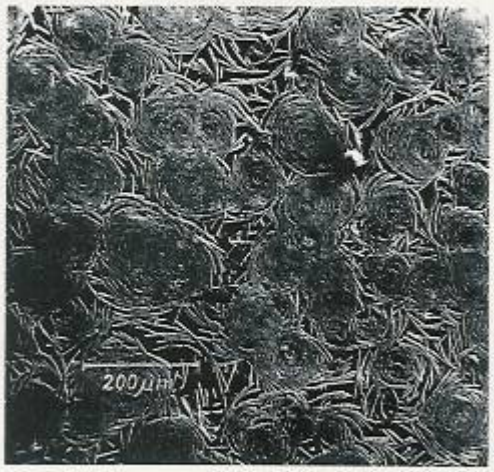

a)

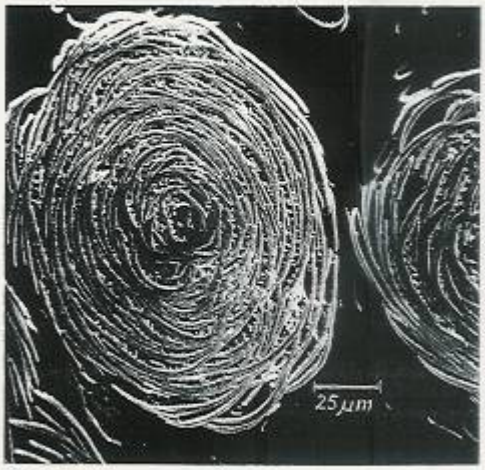

b)

Fig. 4. a) Fluorophlogopite mica crystals in a new configuration. The mica flakes occur in the form of spherically arranged lamellae (cabbagelike). b) A single spherical aggregate (scanning electron micrograph).

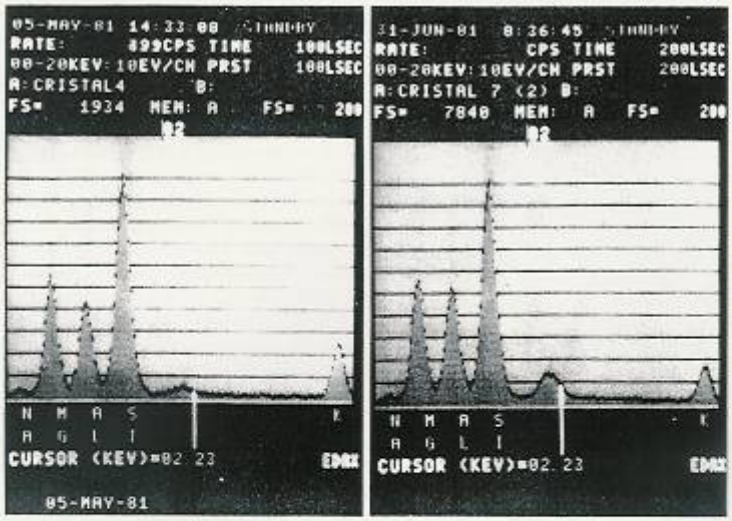

a) b)

Fig. 5. a) EDAX spectra of flat fluorophlogopite mica crystals. Mass ratio Al/Si = 0.43, Mg/Si = 0.71. b) EDAX spectra of curved fluorophlogopite mica crystals. Mass ratio Al/Si = 0.51, Mg/Si = 0.63.

in the octahedron layer of the mica structure, which cause the crystal to bend. This state is also reflected in the change of the dioctahedron–trioctahedron character of the crystals as shown by X-ray diffraction. If the ($MgO + Al_2O_3$) concentration of the base glass were further increased, cordierite crystals ($Mg_2Al_3[AlSi_5O_{18}]$) would be formed. The [$AlO_{4/2}$] groups of cordierite are stabilized by Mg^{2+} ions. The machinability of the glass ceramic containing curved mica crystals is four to five times better[128,29] than that of the glass ceramic with flat mica flakes described in Section 4.1.

This machinable glass ceramic is once again biocompatible and is suitable for many medical applications. Its main properties are compiled in Table 2.

Table 2. Properties of the best machinable glass ceramic containing curved fluorophlogopite mica crystals. Composition [mol%]: M_2O 5–12 (Na_2O 0–8, K_2O 0–6), MgO 8–17, Al_2O_3 21–36, SiO_2 34–60, F 1–7 [29].

Linear coefficient of thermal expansion (20–400 °C)	50–75 × 10^{-7} K^{-1}
Mechanical flex-cracking resistance	Up to 110 MPa
Hydrolytic class	1–2
Alkali class	1–3
Machinability	Excellent

4.3. Machinable Glass Ceramic from the System Na_2O/K_2O-MgO-Al_2O_3-SiO_2-F with both Mica and Cordierite Crystals[131]

Machinable glass ceramics that only contain mica crystals have already been described. Glass ceramics containing solely cordierite crystals ($Mg_2Al_4[AlSi_5O_{18}]$) are also known.[126] The mechanical strength and fracture toughness of these materials are particularly high. Mica and cordierite crystals can be made to separate out simultaneously in specifically modified base glasses by means of controlled phase separation as described in Section 4.2. Glasses of the following composition were used [wt%]:

SiO_2	43–50	F^-	3.3–4.8
Al_2O_3	26–30	Cl^-	0.01–0.6
MgO	11–15	CaO	0.1–3
Na_2O/K_2O	7–10.5	P_2O_5	0.1–5

The glass ceramics thus obtained exhibited a combination of advantageous properties—good machinability, high mechanical strength, and high fracture toughess. This material is suitable for a wide range of uses in dentistry owing to these properties and because it is totally biocompatible, can readily be polished, has a very low roughness height, can be colored, etc.

Figure 6a shows a typical cordierite crystallite in a technical glass as a glass defect; cordierite-mica crystallization in the new glass ceramic described above is shown in Figure 6b for comparison. The close correlations (transition from the curved phlogopite crystal to the cordierite crystal) are clearly revealed in the figure.

The most outstanding properties of the biocompatible, machinable mica-cordierite glass ceramic are compiled in Table 3.

The three types of glass ceramics described above (see Tables 1–3) and other subtypes that satisfy special requirements can be used as biocompatible materials in science, technology, and medicine.

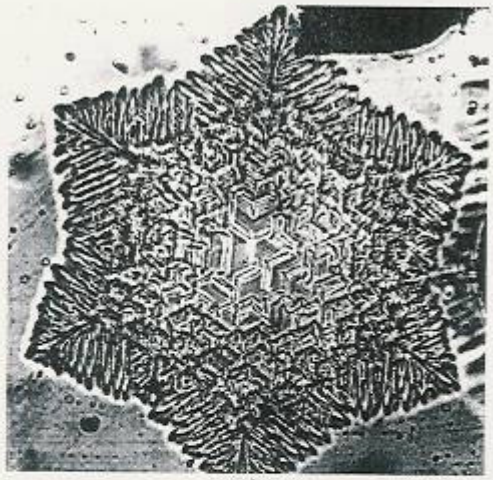

a)

b)

Fig. 6. a) Cordierite crystal as a defect in a technical glass (optical photomicrograph). b) Cordierite crystal in the new machinable glass ceramic that still has curved phlogopite mica crystals (scanning electron micrograph).

Table 3. Properties of the machinable mica (phlogopite)/cordierite glass ceramic.

Density	2.5 g/cm³
Linear coefficient of thermal expansion (20–400 °C)	75–125 × 10⁻⁷ K⁻¹
Mechanical flex-cracking resistance	90–140 MPa
Modulus of elasticity	70 GPa
Pressure resistance	450 MPa
Fracture toughness K_{Ic}	Up to 1.9 Pa · m$^{1/2}$
Vicker's hardness	Up to 8000 MPa
Hydrolytic class	1–2
Acid class	3
Alkali class	1
Roughness height after polishing	0.1 µm
Machinability	Good to very good

5. Development of Bioactive Glass Ceramics

5.1. Machinable, Bioactive Glass Ceramics and the Kinetic Processes Involved in Their Production[32, 33]

The glass ceramics described in Section 4 have proved to be biocompatible and do not disturb living cells. An implant material is generally bioactive if it contains apatite crystals, i.e., the natural building substance of bone.[17, 18, 34] The next logical step, therefore, was to use controlled crystallization to simultaneously segregate both mica (phlogopite) and apatite crystals from a glass melt in variable proportions. In order to understand the procedures used, it should be remembered that controlled phase separation is both the basis of and a prerequisite for almost every controlled crystallization in glass. Phase separation occurs as a result of the formation of stable molecular structural groups and their enrichment in specific regions. As a rule, this considerably facilitates nucleation in the droplet phase since the full amount of the activation energy necessary for a base glass of homogeneous structure is not needed to attain the critical nuclear size. The phase-separation structure of the base glasses in the types of machinable glass ceramics already dealt with has been established. What subsequent steps are required for bioactivity?

5.1.1. CaO and P_2O_5 Doping of the Base Glass from which Fluorophlogopite Mica Crystals Separate Out

When the base glass from which phlogopite crystals separate out is doped with small proportions of CaO/P_2O_5, its phase-separation structure does not change. Figure 7a shows a silicate droplet phase in which Mg, Al, alkali metal, and fluoride ions along with silicic acid are enriched;

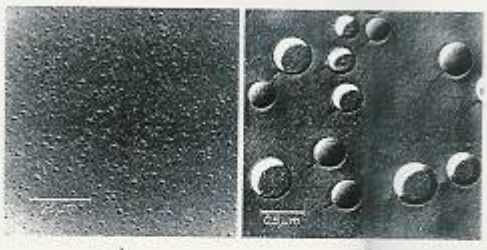

a) b)

Fig. 7. a) Phase-separation structure of the low CaO/P_2O_5-doped base glass after rapid undercooling. Small silicate droplets. b) Phase-separation structure of the high CaO/P_2O_5-doped base glass. Large phosphate droplets. The small silicate droplets have disappeared (replica electron micrograph).

the matrix phase, on the other hand, is very rich in SiO_2. Doping the same base glass with high proportions of CaO/P_2O_5 changes its phase separation behavior fundamentally. The silicate droplet phase disappears. Instead, relatively large droplet regions rich in P_2O_5 are formed in the silicate matrix phase (see Fig. 7b). If the two CaO/P_2O_5-doped base glasses are subjected to specific thermal treatment, only the familiar flat phlogopite crystal flakes and not apatite will separate out from the low CaO/P_2O_5-doped glass.

On the other hand, only apatite separates out from the high CaO/P_2O_5-doped glass; phlogopite crystals do not separate out simultaneously. This apparently negative result is due to the different phase-separation kinetics of the two doped base glasses (see Fig. 8).

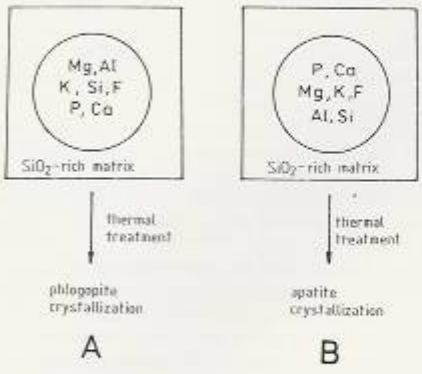

Fig. 8. Schematic representation of phase separation and crystallization kinetics in the glasses shown in Fig. 7.

In case A, most of the low CaO/P_2O_5 content is taken up homogeneously by the droplet phase without fundamental alteration of the familiar crystallization behavior. In case B, where CaO/P_2O_5 doping is high, a pure phosphate droplet phase enriched with Ca^{2+}, Mg^{2+}, Al^{3+}, K^+/Na^+, and F^- is formed in the solidified base glass. The P^{5+} ion has a higher field strength (z/a^2, where z is the valency and a is the distance between the anion and the cation) than the Si^{4+} ion (2.1 and 1.57, respectively); the P^{5+} ion therefore has a greater shielding tendency. A large proportion of the Mg^{2+}, Al^{3+}, and alkali-metal ions are consequently removed from the original silicatic droplet phase so that it disappears in favor of the phosphate droplet phase.

This process is promoted by increasing the fluorine content of the base glass because of a pronounced reduction of viscosity. If this base glass is tempered, only apatite crystallizes. The conditions required for simultaneous separation of phlogopite have been lost.

5.1.2. *CaO (10–19 mol%) and P_2O_5 (2–9 mol%) Doping of the Base Glass from which Spherical, Lamellar Aggregates of Phlogopite Crystals Separate Out*

Doping a base glass having a high Mg^{2+} and Al^{3+} ion content (see Section 4.2) with CaO and P_2O_5 primarily yields a three-phase glass (see Fig. 9a). Two droplet phases with different dimensions and compositions are embedded in a matrix glass phase that is very rich in SiO_2.

The large droplets constitute a phosphate phase that is enriched with MgO, Al_2O_3, K_2O/Na_2O, and F^-. The small droplets are also rich in MgO, Al_2O_3, Na_2O/K_2O, and F^- and represent the original silicate separation phase, which thus still coexists with the phosphate droplet phase.

a) b)

Fig. 9. a) Three phase base glass. Large phosphate droplets and small silicate droplets coexist. b) The large phosphate droplets start to become transformed into apatite crystals (scanning electron micrograph).

In a standard base glass from which flat mica flakes separate out, the addition of phosphorus causes the formation of a new phosphate droplet phase and the distribution ratio for the Mg^{2+}, Al^{3+}, Ca^{2+}, fluoride, and alkali-metal ions is shifted considerably toward the phosphate phase. The silicate droplet phase disappears.

In the case of a base glass with a high MgO and Al_2O_3 content that separates out spherical, lamellar aggregates of phlogopite mica flakes, the basic aim of doping with CaO/P_2O_5 is to obtain the same change in the distribution of Mg^{2+}, Al^{3+}, fluoride, and alkali-metal ions as is found in the standard base glass. The ratio does not, however, favor the phosphate droplet phase so extremely. Owing to the high MgO and Al_2O_3 content of the base glass, sufficient Mg^{2+}, Al^{3+}, F^-, and alkali-metal ions remain in the original silicate droplet phase so that now both droplet phases can exist side by side (see Fig. 9a).

When this type of three-phase glass is tempered, fluoroapatite is formed in the large phosphate droplets. The small silicate droplets still contain enough Mg^{2+}, Al^{3+}, fluoride, and alkali-metal ions to permit formation of phlogopite mica crystals by reaction with the matrix phase. Since, however, the higher field strength of the P^{5+} ions compared with that of the Si^{4+} ions withdraws Mg^{2+}, Al^{3+}, fluoride, and alkali-metal ions from the silicate droplet phase, the mica crystals no longer separate out as lamellar spheres—they revert to the flat flake form. In Figure 9b, the large P_2O_5-rich droplets are beginning to be transformed into apatite crystals whose faces can already be discerned. Figure 10 shows apatite crystals together with fluorophlogopite crystals. The ratio of apatite to phlogopite crystals and the ratio between the residual glass phase and the crystalline phases can be varied. Although the machinability of the glass ceramic is reduced by the simultaneous formation of apatite crystals along with mica crystals, it is still adequate. A major part of the goal outlined at the outset has thus been successfully accomplished in the form of a base glass with the following composition [mol%]:

SiO_2	19–54	F^-	3–23
Al_2O_3	8–15	CaO	10–34
MgO	2–21	P_2O_5	2–10
Na_2O/K_2O	3–8		

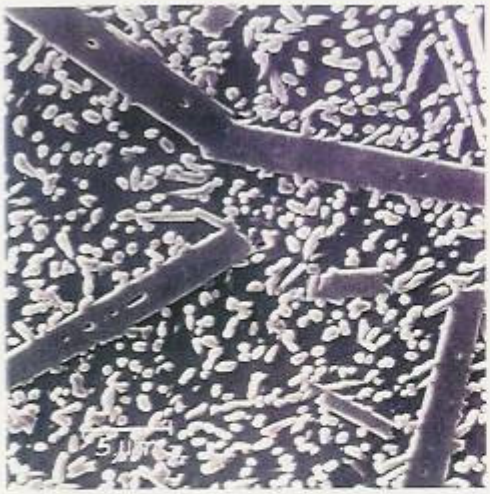

Fig. 10. Bioactive, machinable glass ceramic. Apatite and fluorophlogopite crystals occur side by side in a matrix glass phase (scanning electron micrograph).

5.1.3. Chemical and Mechanical Properties

The behavior of the surfaces of bioglass ceramics toward chemical agents is of particular interest with regard to their possible uses. In the standard water resistance test,[28] the bioglass ceramic optimized for medical applications was found to belong to the "hydrolytic class" 1–2. Machinable glass ceramics with a high apatite content belong to the "hydrolytic class" 2, whereas those with a high phosphate content and a low apatite content are classified in class 3. For comparison, the values for two internationally well-known bioglass ceramics (which are not machinable, however) belong to the "hydrolytic class" 5. The alkali class, determined by standard tests, is I and the acid class 3. These two properties are of little significance as far as medicine is concerned, however, because the test conditions are not comparable to those existing in the human body.

"Ringer's solution"[29] is a model liquid that resembles human physiological body fluid; it is an aqueous solution containing Na^+, Ca^{2+}, Cl^-, and CO_3^{2-} ions. Samples of the new machinable bioglass ceramic boiled in Ringer's solution for 40 h had a roughness height of only 0.5 µm. Tests to detect possible increases in the Na^+ and K^+ ion concentrations of the "Ringer solution" due to leaching proved to be negative.

Another highly informative method for determining the release of ions from an implant under quasi-physiological conditions consists in treating the powdered bioglass ceramic with "Tris" buffer solution (2-amino-2-hydroxymethyl-1,3-propanediol–HCl–H_2O mixture). The results of these tests are given in Table 4.

Further studies showed that the release of Na^+ and K^+ ions had almost stopped after 14 days and practically came to a standstill after 4 weeks. As has already been mentioned in Section 5.1.2, the properties of machinable glass ceramics containing apatite crystals can be varied within wide limits by changing the ratio of apatite to mica crystals. The machinability grades determined by a drilling test ranged from "machinable" to "excellently machinable." Mechanical flex-cracking resistance was measured using samples resting on three points; values ranged from 140 MPa for glass ceramics with a low apatite content to 220 MPa for samples with a high apatite content. In order to minimize scattering of the measured values, the surface of the sample under test was systematically damaged prior to measurement; this was done by exposing it to the action of SiC granules in a rotating drum. (For mechanical properties see Table 5.)

Table 4. Ion release in bioactive, machinable glass-ceramics during treatment with Tris buffer solutions. Experimental conditions: pH of the buffer solution, 7.4; temperature, 37 °C; 3 g of glass ceramic powder with a particle size of 0.16–0.315 mm; 100 mL of solution; sample was agitated constantly. t = reaction time; the measured ion concentration is given.

Bioglass ceramic	t [h]	Ion concentration [mg · L]		
		Na^+	K^+	Al^{3+}
High apatite content	168	1.0	0.7	—
(apatite 40 vol. %,	336	1.1	0.7	—
phlogopite 20 vol. %)	672	1.8	0.7	—
High phlogopite content	168	1.8	2.1	—
(apatite 20 vol. %,	336	1.9	2.1	—
phlogopite 70 vol. %)	672	2.1	2.1	0.08

Table 5. Mechanical properties of the machinable, bioactive glass ceramic. For composition see Section 5.1.2.

Density	2.8 g/cm³
Linear coefficient of thermal expansion (20–300 °C)	$80–120 \times 10^{-7}$ K^{-1}
Mechanical flex-cracking resistance	140–220 MPa
Modulus of elasticity	77–88 GPa
Pressure resistance	500 MPa
Fracture toughness K_{Ic}	0.5–1.0 MPa m$^{1/2}$
Vicker's hardness	Up to 5000 MPa (500 H V 10)

5.1.4. Biocompatibility and Bioactivity

The results of laboratory tests commonly used in medicine such as the INT reduction test, the LDH release test, and, in particular, cell culture experiments were extremely favorable. In the latter case, the materials were added to the cell cultures in the form of a dust at a concentration of 0.4–3.2 mg/mL. Neither the glass ceramic nor the sintered corundum reference substance was found to have any effect on cell multiplication; the glass ceramic must thus be regarded as being completely biocompatible.

The animal experiments performed by *J. Gummel* and *K.-J. Schulze*[30] yielded further results of critical importance. Double implants of a glass ceramic and sintered corundum were made in each experiment; sintered corundum is known to be absolutely biocompatible.

To assess bioactivity, a series of implants were introduced into the tibial heads of guinea pigs. The animals were sacrificed 8, 12, or 16 weeks later or after up to two years, and the tibial heads were removed and subsequently subjected to special tests.

The shearing strength of the implant-bone boundary was determined by measuring the mechanical force necessary to push out the implant cubes. The values found for glass ceramic implants were on average eight times greater than those for the sintered corundum implants. The maximum values were 5 N/mm^2. Moreover, electron microscopic examination revealed that residues of bone adhered to the forcibly removed glass ceramic implants.

Optical and electron micrographs of the ceramic-bone bond provided further interesting insights. Figure 11 shows an optical photomicrograph revealing the direct bond between the bone and the glass ceramic. It can be seen that the alizarin-stained bone substance grows directly into the glass ceramic implant after only eight weeks. Furthermore, bone cells and a blood vessel are found in the immediate vicinity of the implant. Optimal bioactivity has thus been achieved.

Figure 12 shows an optical photomicrograph of the bone-sintered-corundum contact zone that has also been stained with alizarin for comparison. Even 16 weeks after implantation, no direct bonding with the bone is visible. A gap between the bone and the implant has become filled with a layer of connective tissue. The implant could consequently be pulled out like a cork from a bottle. Sintered corundum is therefore biocompatible but not bioactive.

Figure 13 shows a scanning electron micrograph of the boundary layer between the glass ceramic and the bone.

Fig. 11. Intergrowth between bone and glass ceramic eight weeks after implantation in an animal experiment. There is true intergrowth between the bioactive glass ceramic and the bone (optical photomicrograph taken by Dr. *J. Gummel* after alizarin staining [32]). Translation: Bioaktive Glaskeramik = bioactive glass ceramic; Knochen = bone; Knochenzellen = bone cells; Blutgefäß = blood vessel.

Fig. 12. Bone-sintered-corundum contact zone 16 weeks after implantation in an animal experiment. The implant is encapsulated by a layer of connective tissue (collagen). There is no intergrowth between the biocompatible implant and the bone (optical photomicrograph taken by Dr. *J. Gummel* after alizarin staining [32]). Translation: Sinterkorund = sintered corundum; Knochen = bone; Bindegewebe = connective tissue.

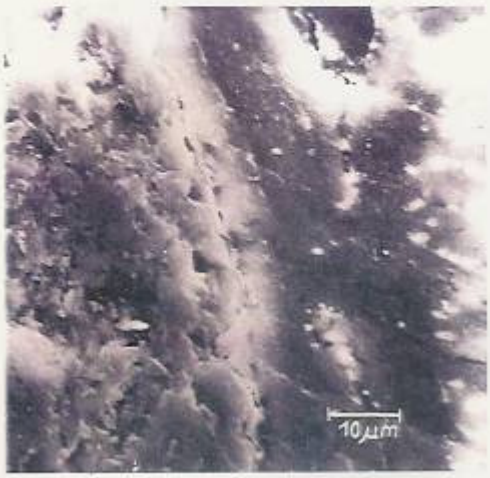

Fig. 13. Intergrowth zone between bioactive glass ceramic and bone in an animal experiment. The maximum thickness of the boundary layer is 5–10 µm (scanning electron micrograph).

Specific dissolution and ion diffusion processes must occur at the surface of the implant under the action of the cell fluid if a firm bond is to be formed between the bone and the implant and new crystals of apatite are to be produced. This dissolution must, however, be brought to a halt at not too great a depth, since the reaction zone will otherwise become too wide which may lead to loosening of the implant if it is subjected to continuous stress later on. Implantation experiments with the new machinable bioactive glass ceramic show that the reaction zone does not exceed 5–10 µm (see Fig. 13). In the case of other foreign bioactive implant materials, the corresponding zone was 100–150 µm and it was not even certain whether the reaction process had completely stopped at the time of examination.

Figure 14 shows an electron-beam microprobe analysis of the boundary layer between the bone and the implant. The X-ray intensity profiles for $Si_{K\alpha}$, $Ca_{K\alpha}$, $P_{K\alpha}$ and $K_{K\alpha}$ radiation suggest the following:

- There is slight leaching of the glass matrix from the surface of the glass ceramic; however, diffusion of SiO_2 into the bone does not occur.
- Leaching of potassium ions from the implant surface is almost quantitative up to a depth of 5 µm. This confirms the previous statement made concerning the width of the reaction zone.

The Ca and P content is higher in the reaction zone than in the glass ceramic. This indicates that new apatite is formed which results in a firm bond between the bioceramic and the bone. The possibility of further bone crystal growth using substances dissolved from the surface of the implant is not excluded.

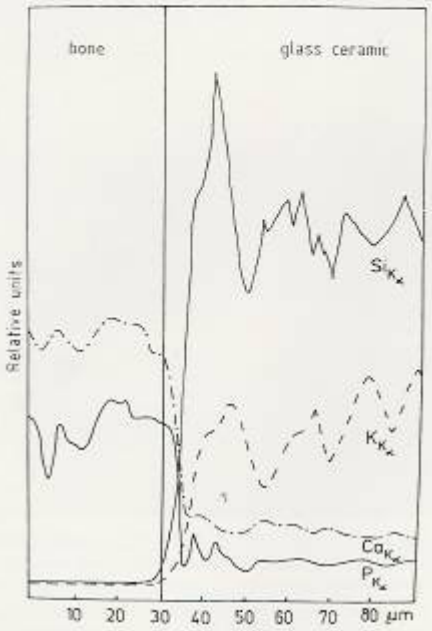

Fig. 14. Electron-beam microprobe investigation of the intergrowth zone shown in Fig. 13. X-ray intensity profiles for $Si_{K\alpha}$, $K_{K\alpha}$, $Ca_{K\alpha}$, and $P_{K\alpha}$ radiation in the boundary layer.

Figures 15a and b show the ceramic–bone bond after 54 and 71 weeks, respectively. The original zone of contact is hardly recognizable, particularly in Figure 15b.

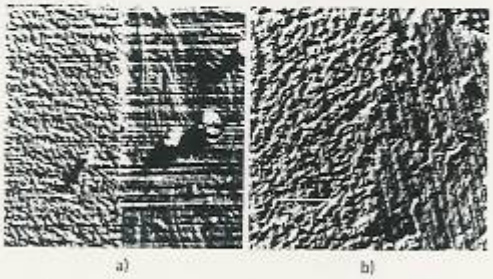

Fig. 15. Scanning electron micrograph of the glass ceramic–bone bond in an animal experiment: a) after 54 weeks; b) after 71 weeks. The contact zone does not broaden as a result of dissolution of the glass ceramic; instead, there is intimate intergrowth.

5.1.5. Interim Assessment and Evaluation of Results

Laboratory and animal experiments designed to test the suitability of the machinable, highly bioactive glass ceramic for bone implants and artificial bones have almost been completed. Experiments on several special applications are still in progress.

The first stage of clinical testing on humans has so far yielded solely positive results. The machinable, highly bioactive glass ceramics provide the surgeon with an implant material that can not only be subjected to the normal procedures used for machining metals but can also be fabricated into complex forms. The surgeon himself will be able to make special corrections and changes during an operation.

5.2. Bioactive, Piezoelectric Phosphate Glass Ceramic Devoid of Silicic Acid

5.2.1. Developmental Trends in Phosphate Glass Ceramics

The successful development of biocompatible and bioactive silicate bioglass ceramics and their medical uses have resulted in medical advances and new possibilities for medical treatment.

It is still not totally certain, however, whether prolonged contact of silicate compounds with the human body will produce undesirable reactions or negative interactions. It would thus be much better to replace bone with a pure biophosphate glass ceramic whose chemical composition corresponds more closely to that of bone than do those of all the bioglass ceramics so far developed. Preliminary efforts in this direction have been made.[58, 59]

The preparation of such a material has not yet been fully accomplished, however, because almost all phosphate glasses have a relatively homogeneous base glass structure and do not display the phase separation that is a prerequisite for controlled crystallization. Only "wild" crystallization is thus possible within or at the surface of the material and does not produce the distinctive properties of a "vitroceramic."

In some cases attempts have been made to overcome the natural structural barriers standing in the way of the development of phosphate glass ceramics by using the glass-powder sinter method.[111] This method consists in tempering, sintering, and crystallizing a phosphate glass powder of suitable composition whose particle sizes approximately correspond to the dimensions of the droplet-shaped immiscibility regions in silicate glasses. Crystallization starts mainly from the surfaces of the particles and proceeds inward toward the center of each glass granule. Uniform crystallization with equal-sized crystallites can thus be achieved in the sintered product by selecting a suitable particle size. The product is porous, however, and its mechanical resistance is lower than that of solid glass ceramics. These materials are therefore only of limited use for medicine; the same also holds for the sintered products of pure crystalline apatite.[110]

The main aim of our studies was to find a way of converting a pure phosphate glass into a glass ceramic by

means of controlled crystallization: one crystalline phase had to be composed of apatite, because existing evidence indicated that this material would be bioactive.

5.2.2. Structure and Crystallization Behavior of Phosphate Glasses

Silicate glasses are generally composed of a three-dimensional network of $[SiO_4]$ tetrahedra. The introduction of network-modifying oxides leads to the breaking of oxygen bridges in the $[SiO_4]$ tetrahedron network and results in the incorporation of the large network-modifying ions in the large network cavities consequently formed (see Fig. 16a).

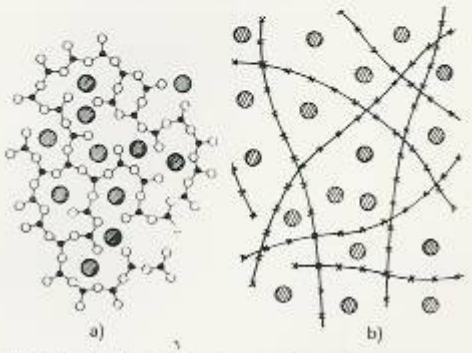

Fig. 16. Hypothetical models for the structure of a) a silicate glass having a network structure; ● = Si, ○ = O, ◎ = Na (according to *Zachariasen* and *Warren* [3]) and b) a basic phosphate glass having a chain structure; × = x, PO_4, ◎ = Na.

In many cases, however, the network-modifying ions are not distributed statistically within the three-dimensional network. Phase separation occurs owing to the different volume requirements of two different molecular building units, one of which tends to concentrate in one microphase and the other in another such phase.[3]

To some extent, the above phenomena can be compared, on the one hand, with mixed crystal formation in analogy with a homogeneous glass and, on the other hand, with a eutectic crystal mixture in analogy with a glass undergoing microphase separation. As has already been discussed in Section 2, however, microphase separation of a glass is of critical importance for controlled crystallization. The structure and thus the crystallization behavior of phosphate glasses differ from those of silicate glasses. Acidic phosphate glasses also consist of a network, but only three corners of each $[PO_4]$ tetrahedron are linked with neighboring tetrahedra. Basic phosphate glasses, especially those with a network-modifying oxide : P_2O_5 ratio > 1 have a chain structure[40–42] (see Fig. 16b). The cavities between tangled chains are so large, however, that they can easily accommodate a different molecular building block of the glass. A tendency to undergo phase separation is therefore not observed. It is thus impossible to use the customary approach to satisfy the criteria for controlled crystallization in these glasses. Other ways must be found.

5.2.3. Development of Pure Biophosphate Glass Ceramics[16, 17]

Glasses of the system CaO-Al_2O_3-P_2O_5: Melts of the ternary system CaO-Al_2O_3-P_2O_5[43] can solidify to form a glass within limited ranges of composition. The ^{31}P-NMR studies of *Haubenreisser* et al.[44], in particular, have clearly demonstrated the chain structure of these glasses. Tempering brings about surface or wild crystallization in which the $AlPO_4$, $Ca(PO_3)_2$, and $Ca_2P_2O_7$ crystalline phase is formed. Apatite does not separate out.

Glasses of the System Na_2O-CaO-Al_2O_3-P_2O_5 and Na_2O-CaO-Al_2O_3-P_2O_5-F: The chain structures of the system CaO-Al_2O_3-P_2O_5 can be specifically degraded by adding increasing amounts of Na_2O; this must improve the chances for the subsequent separation of apatite.

That all of these glasses are "invert glasses" with a P_2O_5 content of less than 50 mol% can be seen from the compositions of the melts [mol%]:

Na_2O	11.0–32.0	Al_2O_3	8.3–16.0
CaO	21.0–37.5	P_2O_5	29.9–42.0

The structural groups determined in the ^{31}P-NMR studies of *Haubenreisser* et al.[44] are solely mono- and diphosphate groups.

In 1959 *Trapp* and *Stevels* were the first to demonstrate the tendency of silicate melts with less than 50 mol% of SiO_2 to form glasses without a three-dimensional network, which they referred to as "invert glasses."[45] The results discussed here indicate that a similar situation may exist in phosphate glass melts. Hypothetical models for the structures of these glasses are presented in Figure 17.

Fig. 17. Hypothetical model for the structure of a phosphate invert glass. Triangles, $[PO_4]$ tetrahedra; black circles, cations (Na^+, Ca^{2+}, Al^{3+}).

Invert glasses, i.e., glasses that are composed exclusively of very small molecular structural groups, tend to crystallize much more rapidly. It was hoped that this would perhaps provide a new way of achieving controlled crystallization in phosphate glasses.

After special thermal treatment, the following crystalline phases can be induced to separate from the above-mentioned glasses: the cristobalite-isotype $AlPO_4$ modification, the tridymite-isotype $AlPO_4$ modification, β-$Ca_2P_2O_7$, an unknown "complex phosphate," a diphosphate, and apatite. However, the crystallization is wild. Most important, a modified hydroxylapatite phase has been made to separate for the first time.

Considerable changes in the crystallization process are observed on addition of fluoride components to melts of the system Na_2O-CaO-Al_2O_3-P_2O_5 [mol%]:

Na_2O	24.1–26.1	P_2O_5	31.6–33.6
CaO	21.7–25.5	F	6.1–10.9
Al_2O_3	11.0–12.2		

Wild crystallization now produces the following crystalline phases: fluoroapatite, the lowquartz-isotype $AlPO_4$ ("berlinite"),[40] which displays piezoelectric properties, and the "complex phosphate phase." ^{27}Al-NMR studies conducted by *Haubenreisser* et al.[44] revealed that the ratio of fourfold- to sixfold-coordinated Al^{3+} was 3:1. This fact, together with the results of the ^{31}P-NMR studies and chemical analyses of the glasses, has been used to deduce a structural model for the "complex phosphate" (see Fig. 18). Such a structural model can indeed be constructed without any strain whatsoever. The precise structure still has to be determined, however. Although controlled crystallization has not yet been achieved in this base glass, attention should be drawn to the special importance of the fluoroapatite and piezoelectric berlinite crystalline phases that have been produced.

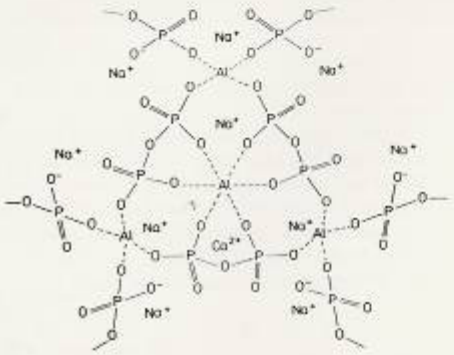

Fig. 18. Hypothetical structure of the crystalline "complex phosphate."

Glasses of the System Na_2O-CaO-Al_2O_3-P_2O_5-FeO/Fe_2O_3 and Na_2O-CaO-Al_2O_3-P_2O_5-F-FeO/Fe_2O_3: Controlled crystallization is not possible in glasses with phosphate chain structures. Phosphate glasses with an invert glass structure (i.e., which contain exclusively mono- or diphosphate structural groups) tend to undergo rapid nucleation and crystallization on tempering. In the corresponding melting diagram, they are located extremely close to the boundary of glass formation. Supersaturation of such melts belonging to the system Na_2O-CaO-Al_2O_3-P_2O_5 with FeO/Fe_2O_3 and cooling or subsequent tempering triggers an effect that resembles phase separation but has nothing at all to do with it.

The selected compositions of the base glasses are [mol%]:

Na_2O	24.1–25.7	P_2O_5	30.7–33.1
CaO	24.9–31.2	FeO/Fe_2O_3	1.2–6.2
Al_2O_3	9.9–14.5		

Figure 19a shows a replica electron micrograph of a selected glass belonging to the system Na_2O-CaO-Al_2O_3-

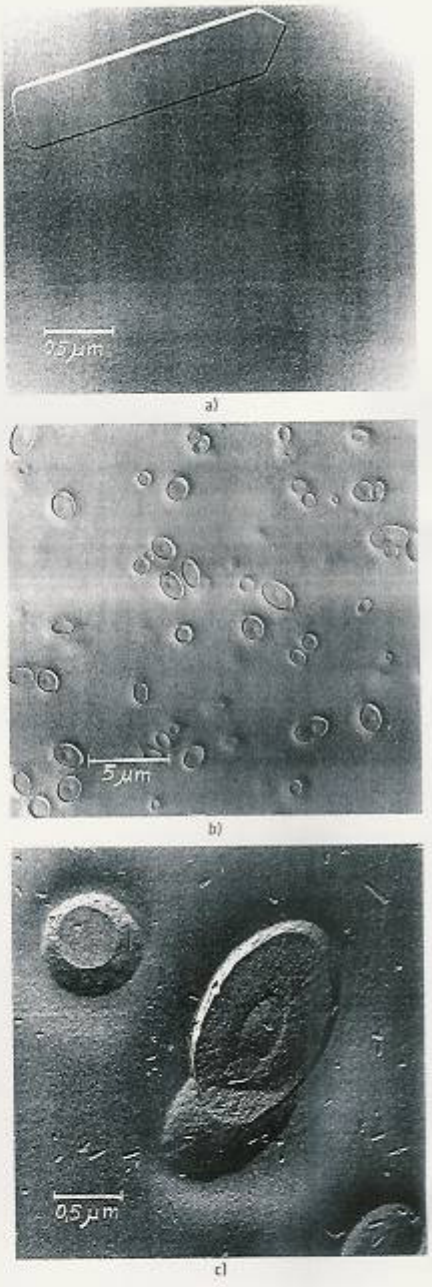

Fig. 19. Replica electron micrograph of a selected glass of the system Na_2O-CaO-Al_2O_3-P_2O_5-FeO/Fe_2O_3. a) After rapid undercooling, the glass displays a homogeneous structure. b) On tempering, supersaturation phenomena disappear; spontaneous nucleation and crystallization occur uniformly throughout the whole glass. c) A single crystallite; a primary iron phosphate nucleus apparently continues to grow by means of epitaxial interaction with the apatite building substance.

P_2O_5-FeO/Fe_2O_3. Comparison of the fractured surface with a MoO_3 crystal test plane clearly demonstrates the homogeneous structure of the glass.

Figure 19b shows a micrograph taken after subjecting the same glass to thermal treatment. Numerous, equal-sized, mostly ellipsoid structures can be seen throughout the glass and are of the kind produced by phase separation. Each ellipsoid region also contains a clearly defined nucleus (see particularly Fig. 19c). The textured structure in Figures 19b and c is a result of the termination of the supersaturation effects because of iron oxides in the base glass.

The nucleus of the ellipsoid region consists of crystalline iron phosphate which has not yet been fully identified. As soon as this primary nucleus has reached a critical size, it apparently continues to grow by means of epitaxial interaction with the hydroxylapatite building substance. Comparison of the lattice constants of apatite with those of various iron phosphates reveals that at least two constants of iron phosphate correspond with two constants of apatite or do not differ by more than ± 15% (see Table 6). In principle, epitaxial interactions are therefore possible; the intermediary formation of iron apatites does not appear to be totally inconceivable either.

Table 6. Comparsion of the lattice parameters of some iron-containing phosphates with those of fluoro- and hydroxylapatite.

Crystalline phase	Lattice parameter [Å]	Difference with respect to apatite [%]
Fluoroapatite	$a = 9.37$	
$Ca_5[F/(PO_4)_3]$	$c = 6.88$	
Hydroxylapatite	$a = 9.43$	
$Ca_5[OH/(PO_4)_3]$	$c = 6.88$	
$Fe_3(PO_4)_2$	$a = 8.80$	− 6.1 to − 6.7 (1 × apatite *a*)
	$b = 11.50$	− 16.4 (2 × apatite *c*)
	$c = 6.25$	− 9.2 (1 × apatite *c*)
$NaFeP_2O_7$ I	$a = 7.11$	+ 3.3 (1 × apatite *c*)
	$b = 10.01$	+ 6.3 bis 7.8 (1 × apatite *a*)
	$c = 8.09$	− 13.7 bis − 14.3 (1 × apatite *a*)
$NaFeP_2O_7$ II	$a = 7.33$	+ 6.5 (1 × apatite *c*)
	$b = 7.90$	+ 14.8 (1 × apatite *c*)
	$c = 9.57$	+ 1.5 bis + 2.1 (1 × apatite *a*)
$Ca_xFe_y(PO_4)_zO_v$ [a]	$a = 9.39$	+ 0.2 bis − 0.5 (1 × apatite *a*)
	$c = 6.90$	+ 0.3 (1 × apatite *c*)

[a] x ≈ 9.5, y ≈ 0.5, z ≈ 1.25.

An X-ray scanning micrograph taken using $Ca_{K\alpha}$ radiation demonstrates the enrichment of Ca in the ellipsoids (see Fig. 20). X-ray diffraction micrographs clearly indicate that the ellipsoids consist of crystalline hydroxylapatite. Further tempering of such glasses leads to the separation of the crystalline "complex phosphate phase" and the tridymite- or cristobalite-like $AlPO_4$ crystalline phase. Figure 21 shows the tridymite-like $AlPO_4$ crystalline phase; interestingly, this phase is extremely similar to the tridymite shape found in silicate glasses. It can also be seen, however, that as the temperature increases, the axes of the star-shaped crystals rearrange to give the cristobalite-like modification of $AlPO_4$ in which the axes intersect at right angles. Equally surprising are the identical appearances of

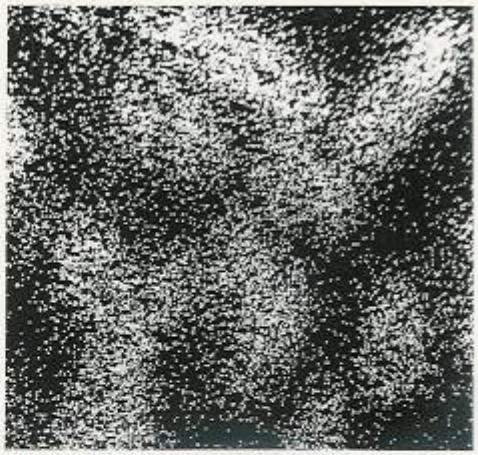

Fig. 20. $Ca_{K\alpha}$ X-ray scanning micrograph of the glass shown in Fig. 19b. Aggregation of Ca^{2+} ions (white dots) in the ellipsoid regions can clearly be seen.

the original cristobalite in silicate glasses and the cristobalite-like modification of $AlPO_4$.

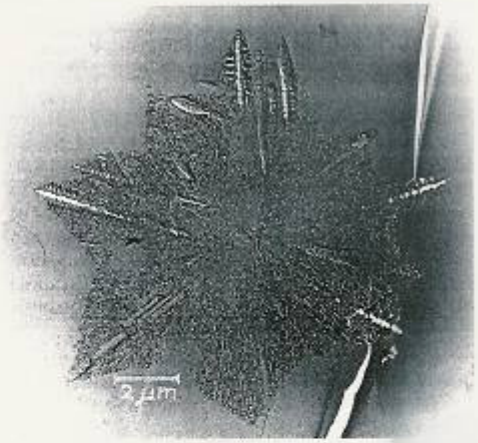

Fig. 21. Formation of the tridymite-like modification of the $AlPO_4$ crystal in the glass matrix obtained after further tempering of the glass shown in Fig. 19b. Transitions to the cristobalite-like $AlPO_4$ modification can be recognized at the ends of the main growth axes of the star-shaped crystal where the axes intersect at right angles (scanning electron micrograph).

A more important advance in attaining optimal bioactivity in phosphate glass ceramics would be achieved if, instead of the cristobalite- or tridymite-like modification of $AlPO_4$, the lowquartz-like $AlPO_4$ modification "berlinite," which exhibits piezoelectric properties,[46] would separate out. In modern medical practice, microcurrents are known to dramatically promote healing of bone fractures.[47,48] Crystallization of apatite and formation of a piezoelectric "berlinite" phase would complement each other very fa-

vorably as regards developing a bioactive pure phosphate glass ceramic.

Separation of "berlinite" can also occur, depending on the fluoride content, in the crystallization of melts belonging to the system Na_2O-CaO-Al_2O_3-P_2O_5-F. It thus seemed logical to add fluoride to melts of the system Na_2O-CaO-Al_2O_3-P_2O_5-FeO/Fe_2O_3 in order to produce the same effect. Separation of "berlinite" has indeed been obtained by adding 2.4–9.4 mol% of fluoride to base glasses of the system Na_2O-CaO-Al_2O_3-P_2O_5-FeO/Fe_2O_3.[106,37]

The complete crystallization sequence occurring during the tempering of certain glasses belonging to the system Na_2O-CaO-Al_2O_3-P_2O_5-F-FeO/Fe_2O_3 is shown in Figure 22. At low temperatures, an iron diphosphate phase and fluoroapatite are formed in addition to the tridymite-like

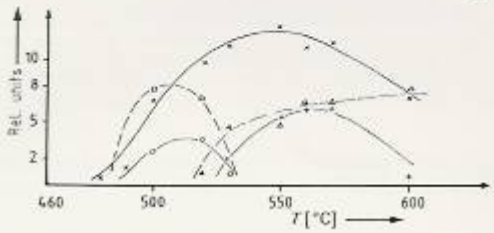

Fig. 22. The temperature dependence of the crystallization sequence of a glass from the system Na_2O-CaO-Al_2O_3-P_2O_5-F-FeO/Fe_2O_3. × — ×, apatite (211); ○ — ○, tridymite-like $AlPO_4$ (1010); + — +, berlinite (102); □ — □, iron diphosphate phase; △ — △, complex phosphate.

$AlPO_4$ modification; the latter decomposes at higher temperatures, however, to form "berlinite." At about 525°C, the crystalline "complex phosphate phase" is formed as well. Figure 22 also shows that an optimal apatite and berlinite content can be obtained at a temperature of approximately 560°C. Thus, a pure phosphate glass with an invert glass structure has been subjected to controlled crystallization (i.e., volume crystallization) by supersaturating it with iron oxides. Fluoroapatite and the piezoelectric lowquartz form of $AlPO_4$ particularly improve the bioactivity of the bioglass ceramic. It is not yet totally clear, however, whether the other crystalline phosphates also contribute to the increase in bioactivity.

5.2.4. Animal Experiments on the Bonding of Phosphate Glass Ceramics and Bone at the Medizinische Akademie Dresden

The first implantation experiments performed in the tibial heads of guinea pigs demonstrated that the bone substance grows into the phosphate glass ceramic without the formation of connective tissue (see Fig. 23). Moreover, microprobe investigations (see Fig. 24) reveal that the bonding zone is only about 10 μm wide and that the dissolution process, which is a prerequisite for intergrowth, stops after about 12 weeks (cf. Fig. 14). The width of the bonding zone in the glass ceramic was taken as being the distance

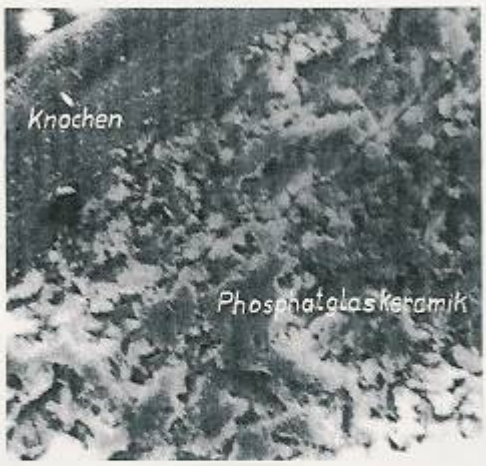

Fig. 23. Intergrowth of pure phosphate glass ceramic and bone in an animal experiment without the formation of connective tissue (scanning electron micrograph). Translation: Knochen = bone; Phosphatglaskeramik = phosphate glass ceramic.

between the point in Figure 24 where the $Ca_{K\alpha}$ intensity suddenly drops and the $Al_{K\alpha}$ intensity simultaneously increases and the point where the $Ca_{K\alpha}$ and $Al_{K\alpha}$ intensities again reach steady levels. If intergrowth is poor or a gap is formed between the glass ceramic and the bone tissue, a totally different microprobe profile is obtained.

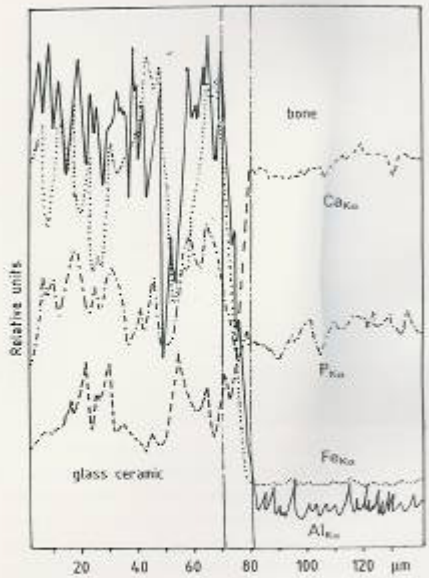

Fig. 24. Electron-beam microprobe profile of the bonding zone in Fig. 23. The zone is not significantly wider than that observed with silicate glass ceramics (cf. Fig. 14).

6. Development of an Inorganic–Organic Bonding Material as a Substitute for Hard Tissue

"Bone cement" is often required in medicine (e.g., to embed endoprostheses or for filling teeth) and usually consists of low-molecular-weight organic compounds that quickly polymerize and harden. Inorganic additives are often mixed with the organic components yielding composite materials. In keeping with more recent applications (e.g., for filling cavities in bones formed during operations), the term "bone cement" should be replaced by the more fitting term "moldable hard-tissue substitute."

If the organic compounds used (e.g., methyl methacrylates, polyurethanes, polyamides, epoxide resins) are applied to a fresh wound as monomers or oligomers, however, they may be removed by the blood during the initial phase prior to polymerization. They may then accumulate at other sites where they can have detrimental effects, including a pronounced drop in blood pressure, fat embolisms,[49] and blood clots.[50] Furthermore, non-reacted isocyanate groups or oligomers can react with body fluid, body tissues, blood corpuscles, or individual proteins, undergoing hydrolysis to give metabolites containing amino groups. Aromatic diamines, in particular, are potential carcinogens.[51]

In all cases, the biocompatible or bioactive glass ceramics or other inorganic materials added to the organic compounds were used exclusively as fillers. The optimal particle size for the inorganic filling materials is 40–60 μm. The reaction zone of many known bioactive glass ceramics reaches 150 μm or more during intergrowth; i.e., any bonding of bone to the mixture of filling material and bioceramic particles occurring in the initial phase is virtually cancelled out by complete dissolution of the particles.

A completely new solution to this problem has now been found.[52] A biocompatible, monomer-free, epoxidated, polymeric hydrocarbon is used which consists solely of C, H, and O. It has a mean molecular weight of 2000 to 6000 with 50 to 500 g of epoxide equivalents. After special surface treatment of the bioactive glass ceramic powders or other additives, they are mixed with the highly polymeric compound to form a chemically bonded substance. Since the surface reaction zones formed during intergrowth with the bone only become 5–12 μm wide (see Section 5.1.4), a sufficient amount of the 40–60-μm bioglass ceramic granule remains to allow firm intergrowth. It is possible to control hardening and the resulting properties of the product, which may vary from cartilage-like to bone-hard. There is no limit so far to the range of applications of these new composite materials.

7. Clinical Testing of the New Bioglass Ceramics in Man

A number of the bioglass ceramics described above have been successfully tested in animals by our medical collaborators. Other bioglass ceramics that are intended for more special applications (e.g., in the eye) are still undergoing tests in animals. Four clinics have been given the go-ahead to perform the first level of clinical tests in humans in special cases.

- At the Orthopädische Klinik (orthopedic clinic) of Charité der Humboldt-Universität Berlin, Prof. H. *Zippel*, in collaboration with Dr. *J. Gummel* and Dr. *H. Hähnel*, has supervised the replacement of single vertebrae in several tumor patients with a bioactive, machinable glass ceramic. Figures 25a–c show several views of a destroyed vertebra before the operation. Figures 25d and e show the substitute vertebra immediately after the operation; it is held in place with a Zielke bridge. The first patient was able to walk without pain after six months.
- At the Hals-, Nasen- und Ohrenklinik (throat, nose, and ear clinic) of the Friedrich-Schiller-Universität Jena, a large range of machinable, biocompatible, and bioactive glass ceramics have been successfully implanted in the middle ear, the nose, the jaw, and the entire skull region (operations performed by Dr. *E. Beleites* under the supervision of Prof. *K.-H. Gramowski*).

The following operations have been performed as part of the first level of clinical tests:

- collumellization in tympanoplasty
- augmentation of the stapes

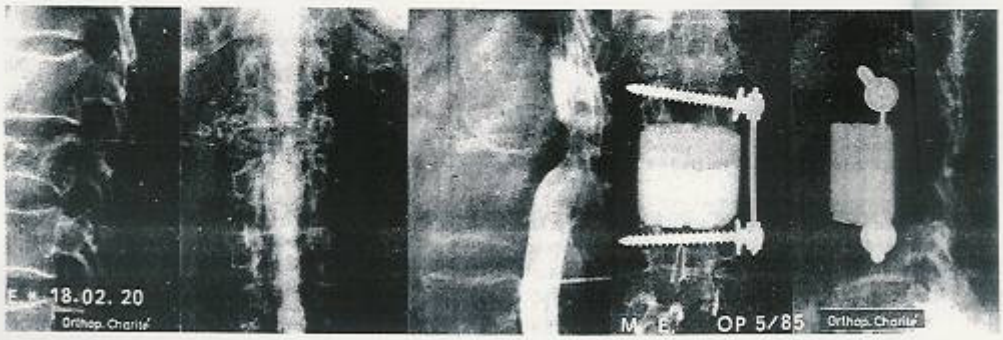

a) b) c) d) e)

Fig. 25. Replacement of a vertebra in a tumor patient with a machinable bioactive glass ceramic (Dr. *J. Gummel*, Charité der Humboldt-Universität Berlin). a)–c) Different views of the destroyed vertebra; d), e) The vertebral prosthesis (X-ray picture). See text.

- reconstruction of the posterior wall of the auditory canal
- reconstruction of the skull base
- maintenance of the base of the orbit
- construction of the anterior wall of the frontal sinus
- rhinoplasty

Figure 26 shows middle-ear implants made by the surgeon. They allowed the patient to hear normally. Animal experiments have demonstrated that intergrowth occurs without causing any adverse reactions and that the biocompatible implant is covered with epithelium. Intergrowth takes place as if the implant were part of the body (see Fig. 27).

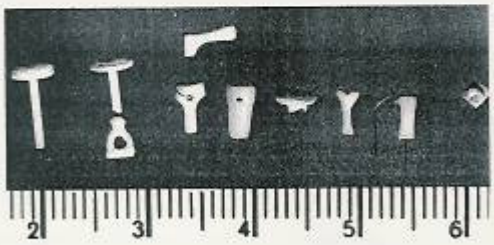

Fig. 26. Middle-ear implants made of machinable biocompatible or bioactive glass that were shaped by the surgeon (Dr. *E. Beleites*, HNO-Klinik der Friedrich-Schiller-Universität Jena). Scale in cm.

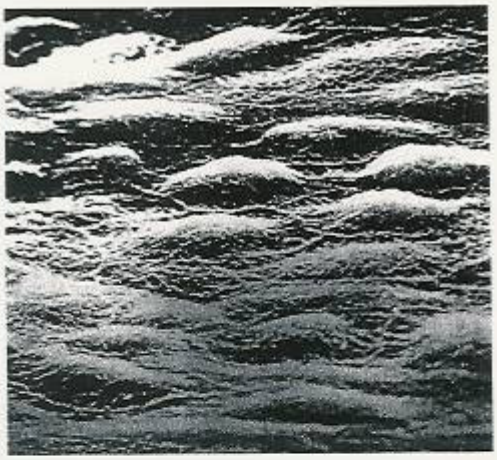

Fig. 27. Intergrowth of an implant made of biocompatible, machinable glass ceramic in an animal experiment. Intergrowth proceeds without causing any irritation and the implant is covered with a layer of epithelium (optical photomicrograph, Dr. *E. Beleites*, HNO-Klinik der Friedrich-Schiller Universität Jena).

— At the Orthopädische Klinik (orthopedic clinic) of the Medizinische Akademie Dresden, machinable bioactive implants have been used for a wide range of applications. The following operations have been performed as part of the first level of clinical tests under the supervision of Prof. *K.-J. Schulze* in collaboration with Dr. *W. Purath* and Dr. *T. Schubert*:

- reconstruction of the root of the acetabulum in a dislocated hip at the dysplasic stage (pericapsular iliumosteotomy according to *Pemberton*)
- ligament fixation in capsule-ligament plastic surgery of the knee joint
- osteotomy of the tibial head and augmentation of the tibial plateau
- operation according to *Bandi*
- partial replacement of vertebrae in the dorsal part of the spine
- ventral spondylodesis in the cervical vertebra according to *Robinson*
- plastic surgery of the shoulder joint according to *Eden-Hybinette*
- distraction osteotomy for keeping of distance
- filling of large bone cysts (glass ceramic as filler)

— Figures 28 and 29 shows two examples for the broad application of machinable, bioactive glass ceramics at the Orthopädischen Klinik der Medizinischen Akademie Dresden.

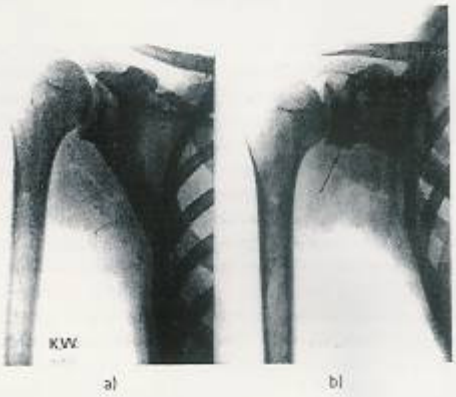

Fig. 28. Use of a wedge-shaped implant made of machinable, bioactive glass ceramic for treating recurrent dislocation of the shoulder by an *Eden-Hybinette* operation. a) Preoperative; b) eight months after the operation. Integration into the bone with good clinical results (Prof. *K.-J. Schulze*, Dr. *W. Purath*, Dr. *T. Schubert*, Medizinische Akademie Dresden).

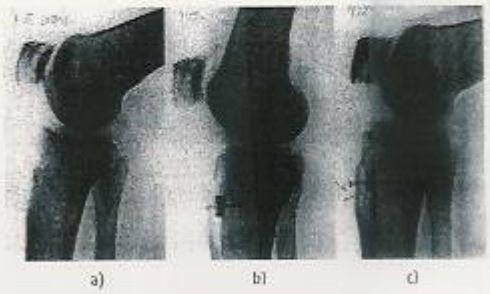

Fig. 29. Use of an oblique, cube-shaped implant made of machinable, bioactive glass ceramic with a central hole and a fixation pin for treating patellofemoral arthrosis by means of ventralization of the tubercle of the tibia according to *Bandi*. a) Preoperative; b) one week and c) eight months after the operation. Integration of the implant into the bone without loss due to correction (Prof. *K.-J. Schulze*, Dr. *W. Purath*, Dr. *T. Schubert*, Medizinische Akademie Dresden).

— At the Klinik und Poliklinik für Kiefer-Gesichts-Chirurgie und Chirurgische Stomatologie (clinic and polyclinic for oral and facial surgery and surgical stomatology) of the Sektion Stomatologie of the Medizinische Akademie Dresden, dental roots have been replaced with machinable, highly bioactive glass ceramics following the successful completion of experiments on pigs performed by Doz. Dr. *R. Pinkert*. The preliminary results are extremely encouraging. Figure 30 shows some of these crude dental root implants; they are made from liquid glass by using a centrifugation technique and are later ceramicized. They were made from an impression of the original after preparing a ceramic mold by means of the centrifugation technique.

Fig. 30. Crude dental root implants made of machinable, highly bioactive glass ceramic. The implants were prepared by a centrifugation technique (Doz. Dr. *R. Pinkert*, Medizinische Akademie Dresden).

8. Summary and Outlook

Considerable progress has been made in this young, interdisciplinary area of science. Not just one but a whole spectrum of bioglass ceramics are now available for medical uses. The properties of these materials can be varied and adjusted within wide limits to suit special medical requirements and different types of applications. However, many questions have not yet been satisfactorily answered: What happens to a bioglass ceramic/bone contact and intergrowth on the long-term scale or when subjected to heavy, variable mechanical loads? How does the gum covering the jaw bone react to dental root implants? As far as prolonged contact is concerned, positive results have been obtained in animal tests extending over several years.

New, unpredictable problems sometimes arise during animal or clinical tests. It can be concluded, however, that the materials have not so far failed in any of their clinical applications. This has encouraged us to pursue further the current direction of development.

One of the advantages of the machinable bioglass ceramics in medicine that is repeatedly stressed is that an implant can be modified and fitted by the surgeon with his own instruments during the course of an operation. This is very important, for instance, in emergency surgery, oral surgery, and stomatology. One of our major aims is to increase the mechanical and shearing resistance of bioglass ceramics either directly or indirectly so that hip joint prostheses can be constructed. It is not yet possible to say whether this goal can be realized. It is evident, however, that the new opportunities for medical treatment that are offered by the development and utilization of new inorganic biomaterials in medicine are by no means exhausted.

The authors would finally like to thank their many co-workers and collaborators for their active and constructive cooperation. It is impossible to mention them all here but several at the Friedrich-Schiller-Universität Jena deserve special mention for their work on the development of biomaterials: Dr. K. Naumann, Dr. J. Vogel, Dr. G. Carl, Dipl.-Chem. P. Wange, Doz. Dr. habil. W. Götz (X-ray crystallography), Dr. G. Völksch and Ing. L. Horn (electron microscopy), Dr. sc. nat. Haubenreisser (nuclear magnetic resonance studies), Prof. Dr. habil. G. Heublein and Dipl.-Chem. M. Böse (organic polymer development). The numerous animal experiments and clinical tests performed by the following medical colleagues have made a decisive contribution to the present status of development: Dr. sc. med. J. Gummel (Humboldt-Universität Berlin), Dr. med. E. Beleites (Friedrich-Schiller-Universität Jena), Prof. Dr. sc. med. K.-J. Schulze (Medizinische Akademie Dresden), Dr. med. T. Schubert (Medizinische Akademie Dresden), Dr. med. W. Purath (Medizinische Akademie Dresden), Doz. Dr. Dr. sc. med. R. Pinkert (Medizinische Akademie Dresden). Our thanks also go to many other medical colleagues whose studies are still at the stage of laboratory and animal tests. Many of our own co-workers—research students, laboratory assistants, and technicians—have also made considerable contributions to the success of the work presented here.

Received: October 6, 1986 [A 621 IE]
German version: *Angew. Chem.* 99 (1987) 541
Translated by Dr. *Gail Schulz*, Seeheim-Jugenheim

[1] W. Vogel, *Angew. Chem. 77* (1965) 109; *Angew. Chem. Int. Ed. Engl. 4* (1965) 112.
[2] W. Vogel: *Struktur und Kristallisation der Gläser*, VEB Deutscher Verlag für Grundstoffindustrie, Leipzig 1965; 2nd ed. 1971; 3rd. ed., *Structure and Crystallization of Glass*, Edition Leipzig, Pergamon Press, Oxford 1971.
[3] W. Vogel: *Glaschemie*, VEB Deutscher Verlag für Grundstoffindustrie, Leipzig 1979; 2nd ed. 1982; 3rd. ed., *Chemistry of Glass*, American Ceramic Society, Columbus, OH (USA) 1985.
[4] C. G. Pantano, E. A. Clark, L. L. Hench, *J. Am. Ceram. Soc. 57* (1974) 412.
[5] M. Ogino, F. Ohuchi, L. L. Hench, *J. Biomed. Mater. Res. 14* (1980) 55.
[6] M. Ogino, L. L. Hench, *J. Non-Cryst. Solids 38/39* (1980) 673.
[7] S. Köhler, K. Reinemeyer, G. Berger, R. Carow, R. Meyer, *Dtsch. Gesundheitsw. 35* (1980) 1343.
[8] R. L. Hentrich, G. A. Graves, H. G. Stein, *J. Biomed. Mater. Res. 5* (1971) 25.
[9] K. Köster, H. Heide, *Z. Orthop. 115* (1977) 604.
[10] M. Akao, H. Aoki, K. Kato, *J. Mater. Sci. 16* (1981) 809.
[11] Zhu Peinan, Cheng Zongquion, Huang Jianong, Sim Quinlian, Feng Meizhen, Chien Pufan, Yang Quinghung, Cai Tidong, *J. Non-Cryst. Solids 52* (1982) 503.
[12] F. Pernot, J. Zarzycky, F. Bonnel, P. Rabischong, R. Baldet, *J. Mater. Sci. 14* (1979) 1694.
[13] T. Kokubo, M. Shigematsu, Y. Nagashima, *Bull. Inst. Chem. Res. Kyoto Univ. 60* (1982) 260.
[14] T. Kokubo, S. Ito, M. Shigematsu, T. Nakamura, T. Yamamuro, S. Higashi, *XIII. Int. Glaskongr.*, Hamburg 1983.
[15] L. L. Hench, *J. Non-Cryst. Solids 19* (1975) 27.
[16] L. L. Hench, H. A. Paschall, *J. Biomed. Mater. Symp. 4* (1973) 25.
[17] H. Kiss, DAS 2 349 859 (1973).
[18] H. Brömer, H. Kiss, E. Pfeil, DBP 2 326 100 (1973).
[19] F. Wihsmann, G. Berger, M. Kiesch, *Wiss. Z. Friedrich-Schiller-Univ. Jena Mat.-Naturwiss. Reihe 32* (1983) 553.
[20] V. Thieme, H. Hofmann, H. Heiner, G. Berger, *Z. Exp. Chir. 15* (1982) 310.

[21] S. Köhler, K. Reitemeyer, G. Berger, R. Kunth, *Silikattech. DDR 34* (1984) 553.
[22] W. Vogel, E. Heidenreich, R. Eltz, DDR-Wirtschafts-Pat. 113885 und DOS 2452076 (1973).
[23] G. H. Beall, M. R. Monstieth, P. Smith, *Glas-Email-Keramo-Tech. 22* (1971) 409.
[24] D. G. Grossmann, DOS 2208236 (1972).
[25] G. K. Chyung, G. H. Beall, D. G. Grossmann, *Int. Congr. Glass (Pap.) 10th (Kyoto) 1974, Kongr. Bd. 14/33* (1974).
[26] W. Vogel, W. Höland, *Adv. Ceram. 4* (1982) 125.
[27] W. Vogel, W. Höland, *Z. Chem. 22* (1982) 429.
[28] W. Höland, K. Naumann, H.-G. Seyferth, W. Vogel, *Z. Chem. 21* (1981) 108.
[29] W. Vogel, W. Höland, K. Naumann, DDR-Wirtschafts-Pat. 0153108 (1980).
[30] W. Höland, W. Vogel, W. J. Mortier, P. H. Duvigneaud, G. Naessens, E. Plumat, *Glass Technol. 24* (1983) 318.
[31] G. Carl, K. Naumann, W. Höland, W. Vogel, DDR-Wirtschafts-Pat. 242216 (1985).
[32] W. Vogel, W. Höland, K. Naumann, J. Gummel, *J. Non-Cryst. Solids 80* (1986) 34.
[33] W. Höland, K. Naumann, W. Vogel, DDR-Wirtschafts-Pat. 237728 (1982).
[34] F. Trojer, P. G. O'Connor, H. Tannenberg, DOS 2606540 (1975).
[35] Technische Normen, Gütevorschriften und Lieferbedingungen (TGL) 14809 (DDR).
[36] J. Vogel, W. Höland, W. Vogel, DDR-Wirtschafts-Pat. 259561/1 (1984).
[37] W. Vogel, J. Vogel, W. Höland, P. Wange, 3rd Int. Otto-Schott Kolloquium 1986.
[38] Y. Abe, A. Nagoya, DBP 3142813 (1983).
[39] Y. Abe, M. Hasue, T. Kasuga, H. Ishikawa, N. Shiokai, Y. Suzuki, J. Nakayama, *J. Am. Ceram. Soc. 65* (1982) 189.
[40] J. R. Van Wazer, *J. Am. Chem. Soc. 72* (1950) 644.
[41] J. R. Van Wazer: *Phosphorus and its Compounds, Vol. 1*, Interscience, New York 1958.
[42] A. E. R. Westman, P. A. Gartaganis, *J. Am. Ceram. Soc. 40* (1957) 293.
[43] P. E. Stone, E. P. Egan, J. R. Lehr, *J. Am. Ceram. Soc. 39* (1956) 96.
[44] U. Haubenreisser, J. Vogel, W. Höland, W. Vogel, 3rd Int. Otto-Schott-Kolloquium 1986.
[45] H. J. L. Trapp, J. M. Stevels, *Glastech. Ber. 32* (1959) K_32.
[46] *Landolt-Börnstein, Neue Serie Gruppe III, Band 2*, Springer, Berlin 1969.
[47] J. Nixon, *Brit. Med. J. 290* (1985) 490.
[48] T. Schubert, *Dissertation*, Medizinische Akademie Dresden 1981.
[49] P. Schultz, *Arch. Orthop. Unfall-Chir. 21* (1971) 301.
[50] M. Suzuki, *J. Biomed. Mater. Res. 15* (1981) 697.
[51] N. A. Mohamud: *Physiochemical Aspects of Polymer Surfaces, Vol. 2*, Plenum Press, New York 1983.
[52] W. Vogel, G. Heublein, W. Höland, M. Böse, K. Naumann, G. Carl, J. Vogel, P. Wange, J. Gummel, P. Zinner, E. Beleites, T. Schubert, DDR-Wirtschafts-Pat. 276665 (1985).